Analysis of Magnetic Disturbance due to Paramagnetic Metallic Implant in Magnetic Resonance Imaging

Yanhui Gao[1], Yui Esaki[1], Hiroshi Dozono[1], Kazuhiro Muramatsu[1] and Toru Yamamoto[2]
[1]Department of Electrical and Electronic Engineering, Saga University, 1 Honjo-Machi, Saga 840-8502, JAPAN
[2]Graduate School of Health Sciences, Hokkaido University, Kita-ku, Sapporo 060-0812, JAPAN
gyanhui@cc.saga-u.ac.jp

***Abstract*— A magnetic disturbance is caused when a metallic implant composed of paramagnetic material is placed in the uniform magnetic field of a magnetic resonance imaging (MRI). This magnetic disturbance distorts the image of the metallic implant and body tissues. Very high accuracy is required to calculate this magnetic disturbance using the magnetic field analysis (MFA), because it is only several μmT. In this paper, the effects of the MFA methods, the analysis models, and the analysis conditions on the calculation accuracy of magnetic disturbance are investigated. The calculated magnetic disturbance is compared with that measured under MRI. It is shown that accurate magnetic disturbance can be achieved by using suitable MFA method, analysis model, and analysis condition.**

***Index Terms*—Finite element methods, magnetic analysis, magnetic resonance imaging, paramagnetic materials.**

I. Introduction

Metallic implants composed of paramagnetic materials, such as stainless steel (SUS), Ti, Co-Cr-Mo alloy, etc., are widely used in the medical industry. And magnetic resonance imaging (MRI) [1] is the most commonly used device to visualize the internal structures of the body. Whereas when a patient with a metallic implant is placed in the uniform magnetic field of a MRI, a magnetic disturbance is created due to its magnetization. This magnetic disturbance in MRI causes the imaging artifact [2, 3] that the image of the metallic implant and body tissues is distorted, and it causes trouble for diagnosis for the patient. To investigate the effect of paramagnetic materials on the magnetic disturbance and the reduction of the magnetic disturbance by combining with diamagnetic materials [4-6], using the magnetic field analysis with the finite element method (FEM) [5-7], higher accuracy is required because the magnetic disturbance is much smaller, ppm level (several μmT), compared with the applied field. However, investigation on the calculation accuracy of magnetic disturbances due to paramagnetic material using magnetic field analysis with FEM seems not enough.

In this paper, the effects of the analysis methods (magnetic vector potential $\boldsymbol{A}$ and magnetic scalar potential Ω methods), models (brick and cylinder shapes), and the analysis condition (water region around the specimen) on the magnetic disturbance are investigated. Then, the magnetic disturbance calculated by using suitable analysis method, analysis model, and condition is compared with that measured under MRI.

II. Model Description

Fig. 1 shows a verification model. Only 1/8 region is shown due to symmetry. In the measurement, the cylinder-shape specimen composed of titanium Ti (paramagnetic material, magnetic susceptibility χ=1.6×10^{-4}) with radius of r = 25 mm and length of l =50 mm is placed at the center in a case (125 ×205×130mm) filled with water (diamagnetic material, χ = – 9.0×10^{-6}). The specimen and water are placed in the MRI, in which the uniform flux density B_{x0} = 1.5T is applied in the x-direction, and the magnetic disturbance is calculated and measured [5]. To remove the disturbance from MRI itself, the magnetic disturbance B_d at each point is determined by using the following equation:

$$B_d = B_{xs} - B_{xw} \tag{1}$$

where B_{xs} and B_{xw} are the x-components of flux densities in the water with and without the specimen, respectively. In the calculation, the flux density at the center point O in the water without specimen is used as B_{xw} at present.

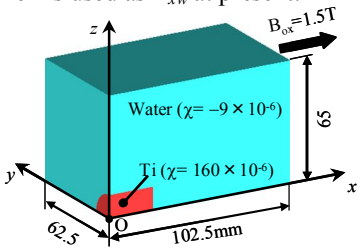

Fig. 1. Verification model.

III. Analysis Method and Conditions

A. Method of Magnetic Field Analysis

The eddy current effect of MRI is removed in the measurement so that linear magnetostatic analyses of $\boldsymbol{A}$ method and Ω methods with the 1st-order hexahedral FEM are performed. Normally $\boldsymbol{A}$ method is applied to electric machine analysis, but it imposes uniform flux on the analysis region. However, Ω method, which imposes uniform field intensity, is considered to be in accordance with the uniform field generated by the coils with constant currents of MRI.

The fundamental equation of the $\boldsymbol{A}$ method is as follows:

$$\mathrm{rot}\left(\nu\ \mathrm{rot}\ \boldsymbol{A}\right) = 0 \tag{2}$$

where ν is reluctivity and the edge element is used. And that of the Ω method is as follows:

$$\mathrm{div}\left(-\mu\ \mathrm{grad}\ \Omega\right) = 0 \tag{3}$$

where μ is permeability and the nodal element is used.

B. Analysis Model

An accurate uniform field cannot be obtained using edge elements when the element shape is distorted. Therefore, the

specimen is modeled with the cylinder shape in the Ω method but with the brick shape shown in Fig. 2(b) in the A method.

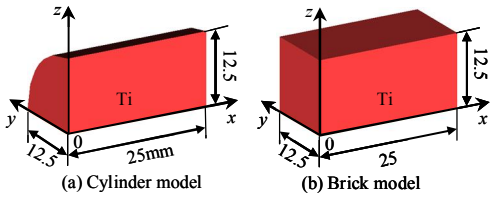

Fig. 2. Shapes of specimen.

C. Analysis Condition

To examine the effect of the water region on the magnetic disturbance, two analysis conditions: the same finite water region with measurement and infinite water region, are investigated.

IV. Results and Discussion

The distributions of B_d in the symmetric plane at y=0 obtained using different methods, models, and conditions are shown in Fig. 3. The solid and dotted lines are the evaluation contour lines of 5ppm.

First, the results using the A and Ω methods are compared in Fig. 3(a). The other common conditions are the brick model and water. The applied flux and magnetic field are given by using the boundary condition in the A and Ω methods, respectively. The discrepancy of using the A and Ω methods is small because it is canceled by subtracting B_{xw} from B_{xs} in (1). However, the difference can be seen clearly as shown in Fig. 4 without subtracting B_{xw} from B_{xs}.

Next, the results using the brick and cylinder models are compared in Fig. 3(b). The other common conditions are the Ω method and water. B_d obtained using the brick model is larger than the cylinder model because the volume of the brick specimen is larger than the cylinder one. Therefore, the model shape should be correctly followed. This means that Ω method should be used by the reason mentioned in III B.

Then, the effect of the water region is examined in Fig. 3(c). The other common conditions are the Ω method and cylinder model. However, B_d becomes larger in the end region of Ti with infinite water region as water is diamagnetic material.

Finally, the distribution of B_d obtained using the suitable analysis conditions, namely, the Ω method, the cylinder model, with finite water region, is compared with measurement result in Fig. 5. It can be concluded that the B_d calculated by using the suitable analysis conditions is in good agreement with the measured one.

The other results will be presented in the full paper.

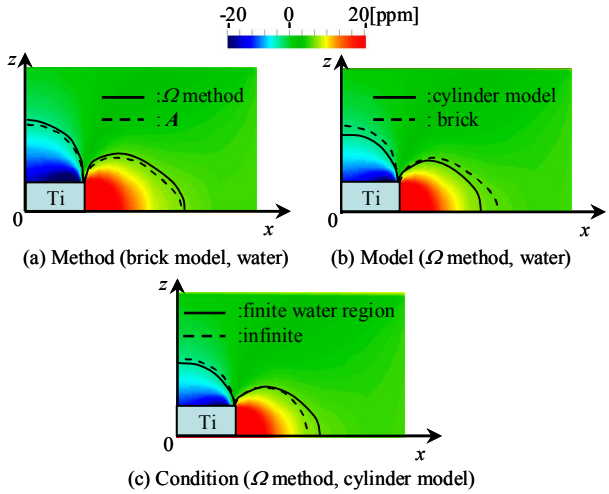

Fig. 3. The effects of analysis conditions on magnetic disturbance at y=0.

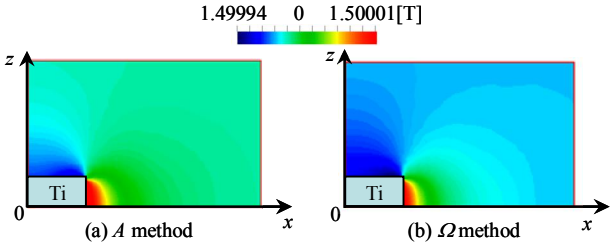

Fig. 4. The effects of analysis methods on magnetic disturbance at y=0 (brick model, infinite water).

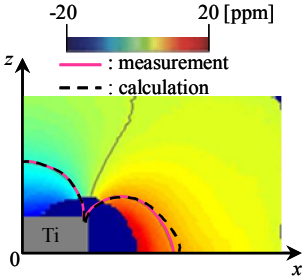

Fig. 5. Comparison of magnetic disturbance between calculation and measurement at y=0.

References

[1] M. E. Mullins, P. W. Schaefer, A. G. Sorensen, E. F. Halpern, H. Ay, J. He, W. J. Koroshetz, and R. G. Gonzalez, "CT and conventional diffusion-weighted MR imaging in acute stroke: Study in 691 patients at presentation to the emergency department," *Radiology*, vol. 224, pp. 353–360, 2002.

[2] A. Ericsson, A. Hemmingsson, B. Jung, and S. Go, "Calculation of MRI artifacts caused by static field disturbances," *Phys. Med. Biol.*, vol. 33, pp. 1103–1112, 1988.

[3] S. Balac and G. Caloz, "Magnetic susceptibility artifacts in magnetic resonance imaging: calculation of the magnetic field disturbances," *IEEE Trans. on Magnetics*, vol. 32, no. 3, pp. 1645-1648, 1996.

[4] B. Chauvel, G. Cathelineau, S. Balac, J. Lecerf, and J. D. de Certaines, "Cancellation of metal-induced MRI artifacts with dual-component paramagnetic and diamagnetic material: Mathematical modelization and experimental verification," *J. Magn. Res. Imag.*, vol. 6, no. 6, pp. 936–938, 1996.

[5] Y. Gao, K. Muramatsu, A. Kushibe, K. Yamazaki, A. Chiba, and T. Yamamoto, "Reduction of artifact of metallic implant in magnetic resonance imaging by coating of diamagnetic material," *IEEE Trans. on Magn.*, vol. 45 , no. 10, pp. 4837-4840, 2009.

[6] Y. Gao, K. Muramatsu, A. Kushibe, K. Yamazaki, A. Chiba, and T. Yamamoto, "Reduction of artifact of metallic implant in magnetic resonance imaging by combining paramagnetic and diamagnetic materials," *Journal of Applied Physics*, vol. 107, no. 9, 09B323-1 - 09B323-3, 2010.

[7] Y. Guo and X. Jiang, "Simulations of the stent artifacts in magnetic resonance imaging," *IEEE Trans. on Magn.*, vol. 48 , no. 2, pp. 659 - 662, 2012.